Charged particles identification using a "telescope" detector

Author	J-M. Fontbonne, J. Dudouet
Address	**LPC Caen, ENSICAEN, Université de Caen, CNRS/IN2P3, Caen, France**
Mail	fontbonne@lpccaen.in2p3.fr dudouet@lpccaen.in2p3.fr

Introduction

So called "telescope" detector assemblies are powerful devices for charged particles identification. They are composed of several detectors (ionization chambers, silicon detectors and scintillators for instance) stacked in order to slow down incident charged particles, the first detector being the thinnest and the last one the thickest.

When an incident charged particle crosses two or more detectors, there is a strong correlation between the energy deposited in each detector. This correlation depends on the mass (A), the charge (Z) and the kinetic energy (E) of the particle allowing the physicist to clearly identify these parameters as we will see in the next paragraphs.

The only requirements for a clear identification (see Fig. 1) are:

- The incident particle losses a "small" amount of energy in the first telescope stages, allowing the measurement of its energy loss (ΔE).
- And come at rest before the end of the last detector, allowing the measurement of its total energy (E).

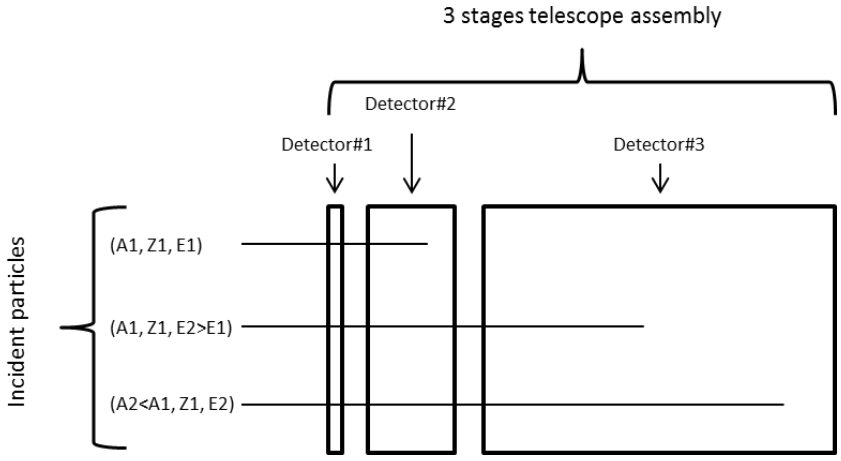

Fig. 1: example of a three stages telescope assembly and particles trajectories for different A, Z, E

What will you find in this educational document?

- An example of "telescope" assembly based on two silicon detecros and a CsI scintillator
- The principles of charged particles identification by using a telescope
- Some simple energy calibration techniques for telescopes
- How to integrate this telescope in the FASTER data acquisition and processing system

J-M. Fontbonne, J. Dudouet, **LPC Caen, ENSICAEN, Université de Caen, CNRS/IN2P3, Caen, France**

1. The device and its electronic

The telescope used for this example has been developed in order to measure energy and identify charged particles coming from the fragmentation of 95A.MeV (=1.14GeV) carbon ions beam on thin targets of mater (essentially hydrogen, carbon and oxygen). The sketch bellow shows the assembly consisting of:

- A thin (150µm) silicon detector providing Si_{thin} signal
- A thick (1000µm) silicon detector providing Si_{thick} signal
- A 10cm thickness Cesium Iodide (CsI) detector coupled to a photomultiplier tube (PM) providing CsI signal

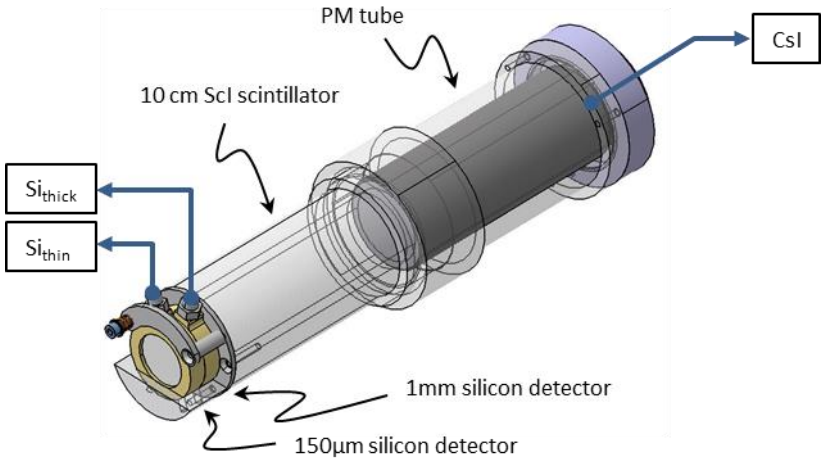

Fig. 2: a telescope example for carbon fragmentation studies

The measurement of energy deposition in the two silicon detectors needs two high quality charge sensitive preamplifiers (CSP) connected to spectroscopy amplifiers and peak hold ADCs. With FASTER, you don't need to cope with the spectroscopy part as the acquisition system contains all the state of the art digital signal processing needed to exploit this kind of signals (but you still have to provide silicon detectors, high voltages and charge sensitive preamplifiers).

- The internal "fast out" signal is used to trigger (threshold discriminator) the acquisition
- The spectroscopy section contains a digital CR-RC4 shaper (variable shaping time) designed for optimum noise charge equivalent measurements (i.e. the lowest possible noise) and a baseline restorer (for EMC purposes). You can select either monopolar output (for optimum noise) or bipolar output (more noisy but less dependent on EMC conditions).

The cases illustrated below were obtained with a monopolar shaping of 1µs time constant.

The use of a CsI scintillator was guided by its aptitude to produces pulse shapes depending on the nature and energy of incident particles. This technique is called pulse shape discrimination (or PSD). As the PM tube generates high level signals, you can integrate the signal over several gate times in order to analyze its shape. To do so, you need a trigger and gate generators enabling charge integrators (QDC). All these devices are provided in FASTER as digital blocs of signal processing.

For this experiment, we used three charge measurements, *Qtot*, *Qfast*, *Qdelayed* repectively gated in the range [-10ns → 10µs], [-10ns → 1µs] and [1µs → 10µs] (time "0ns" being the triggering moment).

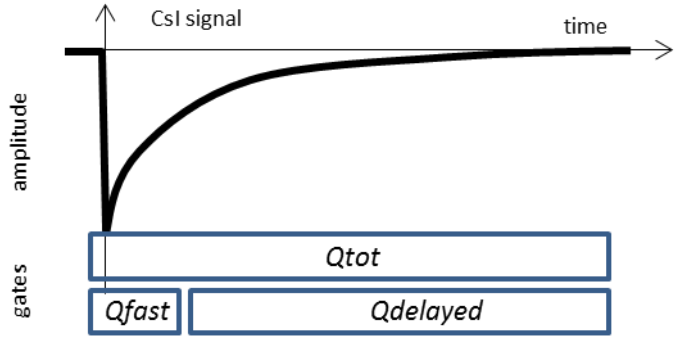

Fig. 3: pulse shape analysis of CsI signal by the mean of three gates

2. Data acquisition:

As spectroscopy usually needs high dynamic ranges, silicon detectors signals should be processed by MOSAHR daughter boards (14bits, 125MHz). The signal coming from the CsI must be sent to a CARAS daughter board (12bits, 500MHz). As mentioned above, FASTER contains all necessary signal processing algorithms you need to get the information a telescope can give. You just have to connect detectors or preamplifiers output to FASTER inputs (see Fig. 4).

Each line of Fig. 4 is triggered independently (depending on the signal magnitude and its presence if the detector is not hit!). As the telescopes were near the target, it was not possible to perform high quality time of flight (that could have helped for off-line event identification/rejection in some cases). Each line was threshold triggered, the threshold being just above the noise floor.

An event was formed and time-stamped when either couples (Si_{thin} and Si_{thick}) or (Si_{thick} and CsI) were triggered.

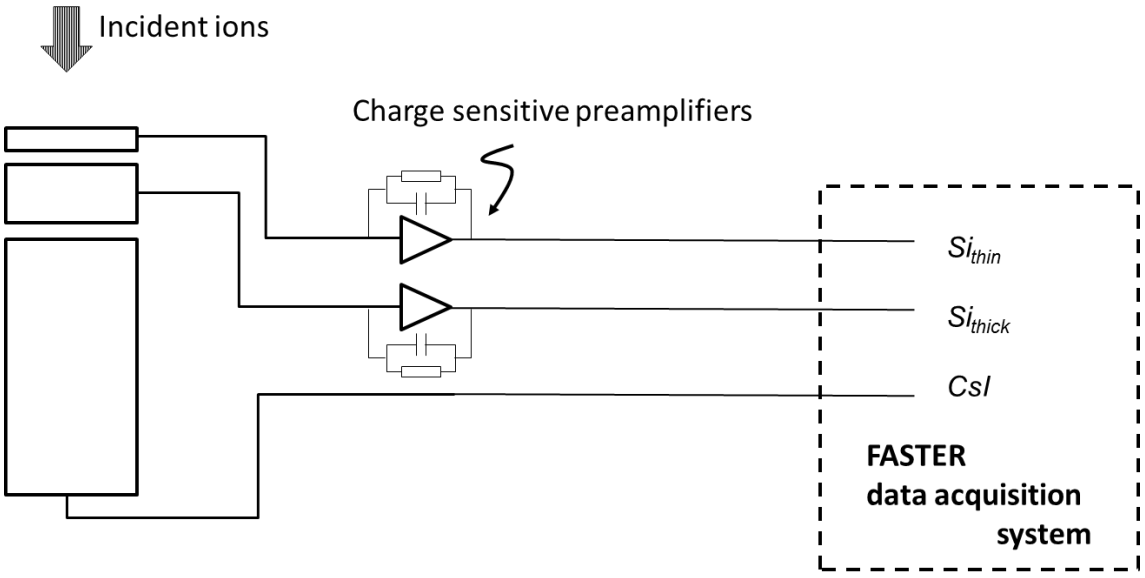

Fig. 4: the complete system for identification and energy measurement of incident ions

3. Data analysis

3.1. Si_{thin} versus Si_{thick}

- *Raw data plotting*

Each time a couple (Si_{thin} and Si_{thick}) triggers the acquisition, it is possible to place a point on a bi-dimensional plot (bidim plot) whose X coordinates corresponds to Si_{thick} value and Y coordinate to Si_{thin} value. When million points are acquired, one obtains the graph shown on Fig. 5.

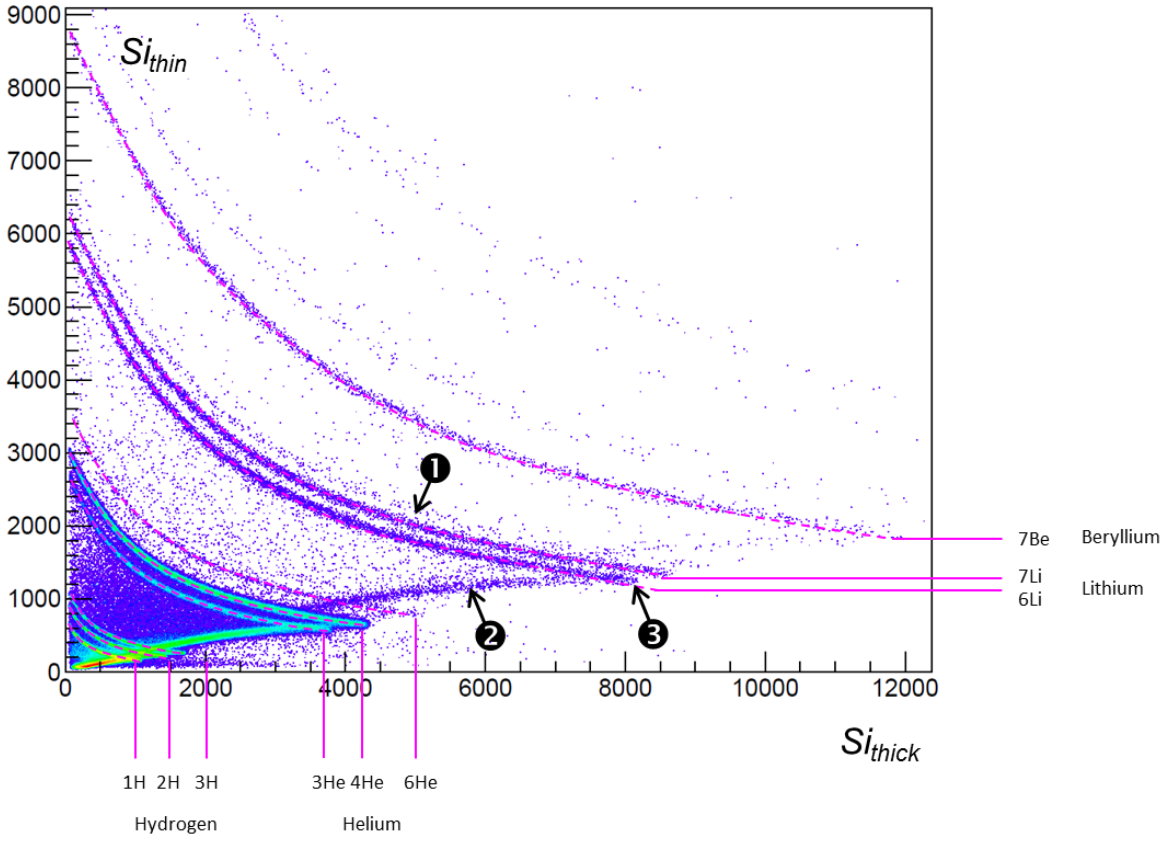

Fig. 5: Bidim plot of Si_{thin} vs Si_{thick} . Axis values in arbitrary units

One clearly sees the contribution of different kinds of particles hitting the two detectors. The graph (Fig. 5) shows hyperbolic (at least curved) structures (1) and quasi straight lines (2) joining the origin to the hyperbolas at a precise cusp point (3).

In fact, when a particle crosses the first detector and comes at rest in the second one, its trace lies in one of the hyperbolas.

The origin of straight lines comes from particles crossing both detectors. They can't be identified this way. This is the reason why we need a third detector stage (see below).

- *Particles identification*

A way to identify the different groups consists on having a look at a "chart of nuclides" as the one of *nndc* (www.nndc.bnl.gov/chart/) for instance. A reprint of the beginning of the chart looks like:

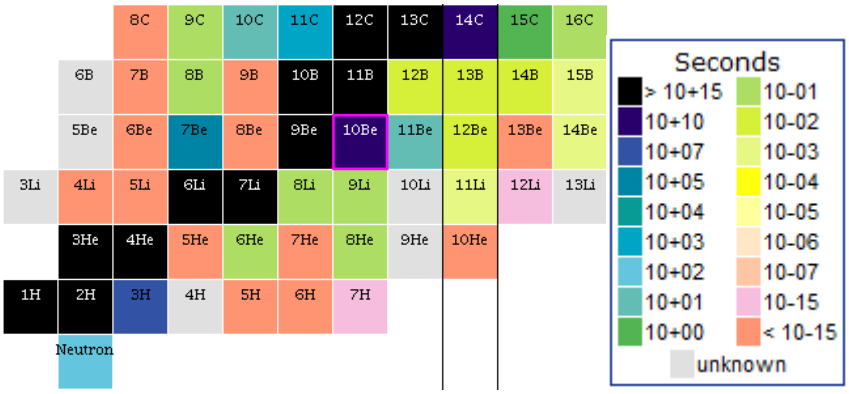

Fig. 6: chart of nuclides from www.nndc.bnl.gov/chart/

The main lines on the bidim plot usually correspond to stable or long life isotopes {[1H, 2H, 3H]; [3He, 4He, 6He]; [6Li, 7Li, 8Li, 9Li]; [7Be, 9Be, 10Be, 11Be]; [8B, 10B, 11B]; [9C, 10C, 11C, 12C, 13C, 14C…]}. What is especially visible on Fig. 5 is the lack of some identification lines corresponding to 5He and 8Be. By "playing" with existing lines and lacking lines, it is possible to create the identification map (plotted in magenta dotted lines on Fig. 6).

- *Energy calibration*

Up to now, we can identify incident particles by their mass and charge. We must now calibrate their energy. By downloading SRIM at www.srim.org/ we have a simple and easy to use tool to perform this job. Let's have a look at the range of 6Li ions in silicon (see Fig. 7).

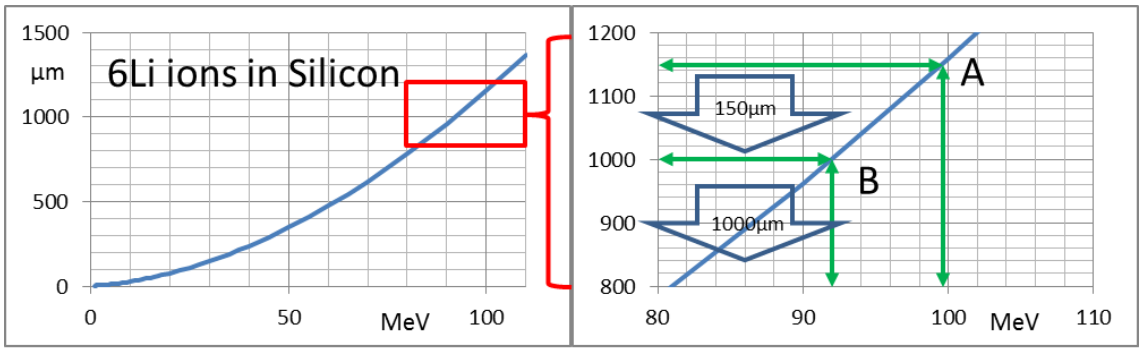

Fig. 7: range versus incident energy for 6Li ions in silicon (left) and a zoom around the region of interest (right)

Fig. 6 exhibits interesting points: for instance, the cusp point (3) of the graph. At these points, we know that the incident particle had just the necessary energy the cross the two detectors (total thickness 150 + 1000 µm) but came at rest before hitting the third one (as it lies exactly on the cusp point). Having a look at Fig. 7.right (point A), we learn that a 6Li particle should have exactly 100MeV energy to travel thru 1150µm of silicon. This is the

energy this particle had at the entrance of the telescope. As the particle exactly travelled 1000µm in the second stage, we learn (point B) that it lost exactly 92MeV in the second detector, so it lost 8MeV in the first one (100 – 92MeV).

The identification map is now calibrated as we know that 8000bins on X axis (Si_{thick}) correspond to 92MeV and 1500bins on Y axis (Si_{thin}) represent 8MeV. Obviously, the same procedure can be applied to the other particles in order to improve the energy calibration.

3.2. Si_{thick} versus CsI

For energetic particles, it's necessary to have a look at the Si_{thick} vs CsI bidim represented below (Fig. 8).

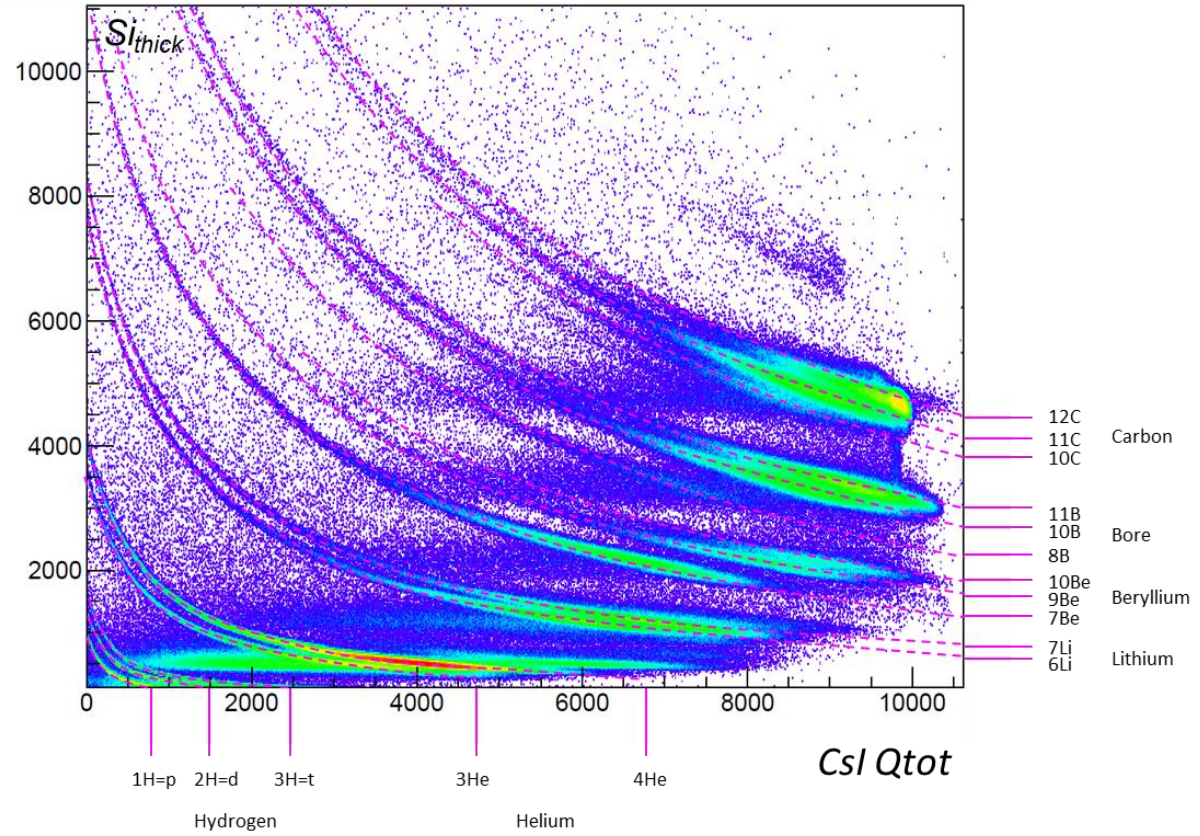

Fig. 8: bidim plot of Si_{thick} vs CsI. Axis values in arbitrary units

We can see the hyperbolas mentioned above but there is no cusp as the CsI scintillator thickness was designed to stop all incident particles (even the lighter and most energetic ones). The identification map goes up to carbon ions and one can see a few nitrogen ions.

The horizontal lines come from particles escaping the CsI detector by its sides.

As we previously calibrated the silicon detector, we don't need to do the job again. In fact, the CsI response is not linear, neither in energy, nor in particle type (contrary to silicon detectors). Fortunately, identification lines remain clearly visible.

3.3. Pulse shape analysis using CsI:

An interesting property of CsI detectors is that, despite their non-linear energy response, they provide internal scintillation mechanisms allowing particle identification as previously mentioned. Analyzing the pulse shape by the mean of two integration gates allow the user to create identification maps for the CsI by itself. In fact, it just consists in plotting the delayed charge versus the fast charge (for instance), as shown on Fig. 9.

If the detector response were perfectly linear, all the points would lie on a straight line (in fact the hydrogen group in this map). The main scintillation mechanisms of CsI detectors are affected by scintillation quenching. The more the linear energy transfer of the incident particle in the scintillator is, the less the linear scintillation production in the detector is. Furthermore, the intensity ratio of "prompt" light and "delayed" light is also affected by this phenomenon. So, particles of same energy, with different A or Z mass are not located the same place in the Qdelayed vs Qfast bidim.

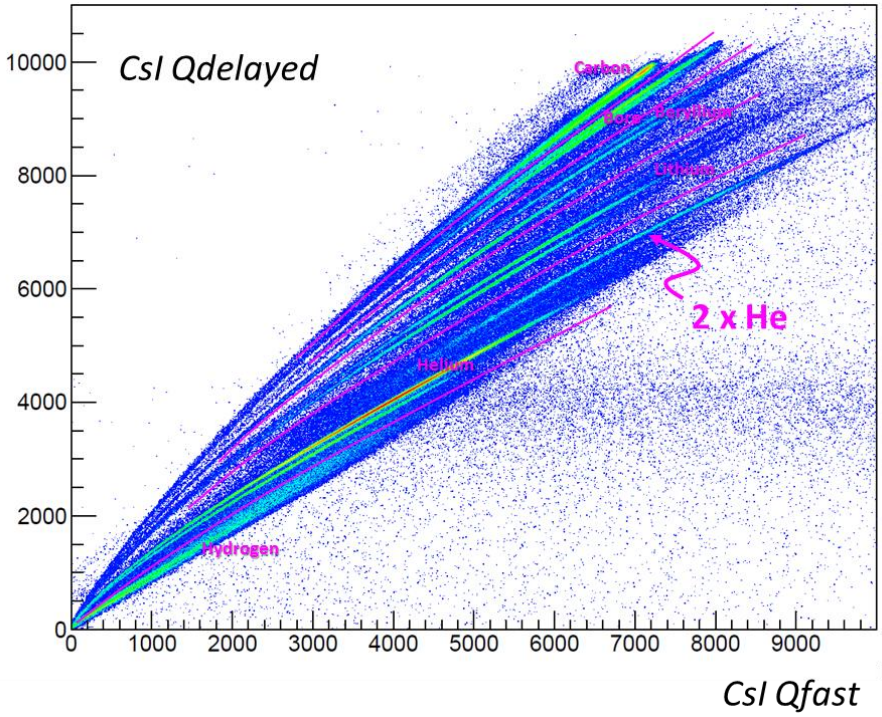

Fig. 9: delayed vs prompt light emission in CsI scintillator

The interesting point in this bidim plot is that information is not spread the same way as in the previous figures. One can see for instance a specific line identified as the

simultaneous interaction of two helium particles in the detector (event buildup or in flight disintegration of short life radioactive ions). This kind of event was not visible, neither in Fig. 5, nor in Fig. 8 and would have led to bad identifications.

4. Conclusions

Telescope assemblies are powerful tools for particles identification and energy measurement. The multiparametric plots allow deep sights inside the event reconstruction of a nuclear physics experiment.

The energy calibration remains the most complicated task of such an exercise. The methods explained above are very simple but a quiet rough. Far more sophisticated technics exist but were not under the scope of this educational document. For more information, please refer to "Jerem's papers".

J-M. Fontbonne, J. Dudouet, **LPC Caen, ENSICAEN, Université de Caen, CNRS/IN2P3, Caen, France**